

Osteoarthritis and Cartilage



Passage-dependent relationship between mesenchymal stem cell mobilization and chondrogenic potential



A.R. Tan †, E. Alegre-Aguarón †, G.D. O'Connell ‡, C.D. VandenBerg §, R.K. Aaron ||, G. Vunjak-Novakovic †, J. Chloe Bulinski ¶, G.A. Ateshian †#, C.T. Hung †*

† Department of Biomedical Engineering, Columbia University, 1210 Amsterdam Ave, New York, NY 10027, USA

‡ Department of Mechanical Engineering, University of California, Berkeley, 5122 Etcheverry Hall, Berkeley, CA 94720, USA

§ Department of Orthopaedic Surgery, St. Luke's-Roosevelt Hospital Center, 1000 10th Ave, New York, NY 10019, USA

|| Department of Orthopaedic Surgery, Brown University, 100 Butler Drive, Providence, RI 02906, USA

¶ Department of Biological Sciences, Columbia University, 1212 Amsterdam Ave, New York, NY 10027, USA

Department of Mechanical Engineering, Columbia University, 500 W. 120th St, New York, NY 10027, USA

ARTICLE INFO

Article history:

Received 1 April 2014

Accepted 6 October 2014

Keywords:

SDSCs

CD73

Galvanotaxis

Cartilage repair

Tissue engineering

SUMMARY

Objective: Galvanotaxis, the migratory response of cells in response to electrical stimulation, has been implicated in development and wound healing. The use of mesenchymal stem cells (MSCs) from the synovium (synovium-derived stem cells, SDSCs) has been investigated for repair strategies. Expansion of SDSCs is necessary to achieve clinically relevant cell numbers; however, the effects of culture passage on their subsequent cartilaginous extracellular matrix production are not well understood.

Methods: Over four passages of SDSCs, we measured the expression of cell surface markers (CD31, CD34, CD49c, CD73) and assessed their migratory potential in response to applied direct current (DC) electric field. Cells from each passage were also used to form micropellets to assess the degree of cartilage-like tissue formation.

Results: Expression of CD31, CD34, and CD49c remained constant throughout cell expansion; CD73 showed a transient increase through the first two passages. Correspondingly, we observed that early passage SDSCs exhibit anodal migration when subjected to applied DC electric field strength of 6 V/cm. By passage 3, CD73 expression significantly decreased; these cells exhibited cell migration toward the cathode, as previously observed for terminally differentiated chondrocytes. Only late passage cells (P4) were capable of developing cartilage-like tissue in micropellet culture.

Conclusions: Our results show cell priming protocols carried out for four passages selectively differentiate stem cells to behave like chondrocytes, both in their motility response to applied electric field and their production of cartilaginous tissue.

© 2014 Osteoarthritis Research Society International. Published by Elsevier Ltd. All rights reserved.

Introduction

Articular cartilage is the connective tissue that lines diarthrodial joints and serves to bear load and provide low friction and wear during motion¹. When the tissue is damaged through physical injury or a disease such as osteoarthritis (OA), the healing response is inadequate due to the avascular nature and limited cellularity of adult cartilage². We and others have investigated the use of

mesenchymal stem cells (MSCs) found in the neighboring synovium, that are known as SDSCs^{3,4}, for the repair of articular cartilage. With the addition of appropriate lineage-specific culture medium, the population of SDSCs has been confirmed to be multipotent, capable of differentiating into several mesenchymal lineages, including chondrocytes, osteoblasts, adipocytes, and myocytes^{5–7}. As such, harvested SDSCs expanded through multiple passages *in vitro* in the presence of a chondrogenesis-promoting growth factor cocktail^{3,4} have been shown to produce extracellular matrix (ECM) components similar to chondrocytes (i.e., collagen II and aggrecan)^{4,6,8} and to generate material and mechanical properties similar to native cartilage when encapsulated in agarose hydrogel³. SDSCs thus represent a promising new source for cell-based strategies for the repair of articular cartilage.

* Address correspondence and reprint requests to: C.T. Hung, Department of Biomedical Engineering, Columbia University, 1210 Amsterdam Ave, New York, NY 10027, USA. Tel.: 1-212-854-6542.

E-mail address: cth6@columbia.edu (C.T. Hung).

The delayed, ultimately poor healing ability of articular cartilage is thought to be due, in large part, to insufficient migration to the damage site by cells that have the potential to repair the lesion⁹. Thus, strategies that enhance and direct SDSC migration could amplify the intrinsic repair process. The use of direct current (DC) electric fields (EFs) of strengths ranging from 1 to 10 V/cm is known to induce directed movement (galvanotaxis) and shape change (galvanotropism) in a number of musculoskeletal cells including chondrocytes, fibroblasts, osteoblasts, osteoclasts, and meniscal fibrochondrocytes¹⁰. Endogenously generated EF gradients of this strength have also been shown to guide cell migration in developing embryos¹¹ and at the cut surface of wounds¹². Hence, galvanotaxis may be a useful tool for encouraging and promoting the migration of a clinically relevant cell type to sites of articular cartilage defects.

Stem cells such as SDSCs exhibit phenotypic and behavioral changes as terminal differentiation is reached. Previously, we determined via flow cytometry, that changes in cell surface molecules are measurable throughout differentiation; some of these surface molecules may in fact serve as growth factor receptors or adhesion molecules that play a direct role in the differentiation process. Further, it was shown that manipulation of cell surface changes with chemical modifiers such as neuraminidase, an enzyme that removes sialic acids¹³, or lectins¹⁴, alters EF motility¹⁵, pointing to a strong influence of surface molecules in directed migration. Taken together, these results suggest the hypothesis that differentiating SDSCs exhibit markedly different behavior depending on culture expansion age.

We are unaware of any previous studies that correlate a change in cell surface marker expression with a change in migration response to EF. Furthermore, it is not clear whether cells of a certain passage are preferentially more likely to adopt a phenotype favorable for cartilage matrix development. Thus, in this paper, we examine the surface markers and migration characteristics of SDSCs through four passages of culture; we hypothesize that as SDSCs reach a chondrocytic phenotype, their migration characteristics begin to resemble those reported for chondrocytes¹⁶. In parallel, through 3D pellet cultures using cells from each passage, we attempt to elucidate the passage at which SDSCs exhibit the greatest potential to synthesize cartilaginous matrix, in order to optimize their use for tissue-engineered constructs.

Methods and materials

Experimental design

Three controlled and concurrent cell culture studies are described herein, aimed at characterizing the behavior of juvenile bovine SDSCs. Specifically, study one examined the effect of cell passage number on the expression of four cell surface markers found on MSCs. Study two characterized the cellular response of these cells at each passage to an applied DC EF of comparable magnitude as those found at the cut surface of wounds in order to identify a cell population most suitable for wound repair. Finally, study three explored the development of tissue at each passage to investigate a potential correlation between cell migration behavior and matrix composition.

Cell isolation and expansion

The intimal layer of the synovium was harvested from bovine knee joints of four freshly slaughtered 2–4 week old calves, as described previously³. Medium supplemented with 1 ng/mL TGF- β 1, 5 ng/mL bFGF, and 10 ng/mL PDGF- β 3³ was changed every three days. At confluence, cells were trypsinized and then counted. One

subset of the cells at each passage was replated for further expansion, another subset was used for flow cytometry analysis, a third subset was used for galvanotaxis experiments, and a final subset was used for 3D micropellet culture.

Cell surface marker assessment

The phenotype of bovine SDSCs at each passage (P1 to P4) was assessed by flow cytometry, as previously described¹⁷. Cells were stained with antibodies against CD31 (endothelial cell marker, Thermo Scientific), CD34 (hematopoietic cell marker, Abcam), and mesenchymal markers CD49c (Thermo Scientific) and CD73 (Bio-Legend)^{18,19}; positive MSC classification requires the absence of CD31 and CD34 and presence of CD73²⁰, while CD49c is a constant marker of chondrogenic potential of MSCs, decreasing only in the presence of TGF- β 3^{21,22}. Cellular fluorescence was evaluated using a FACSCalibur flow cytometer (Becton Dickinson, Franklin Lakes, NJ) and the resulting data analyzed with FlowJo software (version 9.3.2).

Galvanotaxis

After trypsinization, cells were allowed to equilibrate for 1 h before being plated at 2.65×10^4 cells/cm² onto sterile glass slides (Fisher Scientific, Pittsburgh, PA) with removable silicone wells. To investigate the influence of CD73 on P1 cells, one subset of cells was exposed to 100 μ M 5'-(α , β -methylene)diphosphate (APCP)²³, a CD73 inhibitor, during the plating period. After cells were allowed to attach for 1 h in a 5% CO₂ incubator at 37°C, the slide was rinsed with medium to remove any nonadherent cells and placed into a custom galvanotaxis chamber under aseptic conditions [Fig. 1, described in Ref. 16].

A power supply (Kiethley Instruments) delivered a current of 3.3 mA (6 V/cm EF strength) through the chamber, and experiments were performed at room temperature for 3 h. Control slides were treated similarly without EF. Cell migration patterns were captured every 10 min using an Olympus IX-70 inverted microscope and digital camera ($n = 30$ –40 cells observed in each field of view).

Cell migration parameters

The position of each cell was manually tracked via a custom MATLAB program^{16,24}. Migration direction was quantified as $\sin \varphi$, where φ is the angle between the x -coordinate axis and the migration vector, such that $\sin \varphi$ was defined as the value -1 when $\varphi = 4.71$ rad (270°), the direction of the cathode. The directional velocity, defined as the component of the speed directed toward the negative pole (e.g., Refs. 16,25), was obtained by multiplying a cell's speed by $\sin \varphi$.

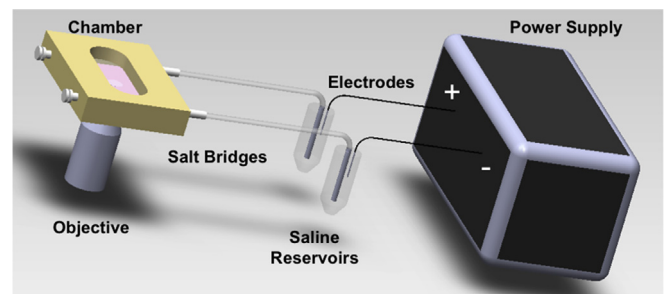


Fig. 1. Schematic of galvanotaxis setup. Cells seeded on a glass slide were inserted into a custom chamber and exposed to an electric field gradient for three hours.

Micropellet culture

Following trypsinization at each passage, cells were counted and 0.5 mL each of a 1×10^6 cell suspension was aliquotted into 1.5 mL sterile screw-top tubes, formed into pellets by centrifugation, and cultured for 42 days. Chondrogenic medium²⁶ was supplemented with 10 ng/mL TGF- β 3 (R&D Systems) for the first 21 days. At days 14, 28, and 42, micropellet samples were harvested. Medium was completely removed and one subset of the micropellets was individually stored at -20°C for biochemical assaying ($n = 5$). The other subset of micropellets was fixed in acid formalin ethanol for immunohistological analysis.

Micropellet immunohistological analysis

Fixed samples were paraffin embedded, sectioned (8 μm thick), and stained for type I and type II collagen, as previously described²⁷, with TOTO-3 nuclear counterstaining to visualize collagen networks and cells. After staining, slides were coverslipped with Fluoroshield (Sigma) and sections were analyzed using an inverted microscope with an Olympus Fluoview confocal system with dual wavelengths excitation at 488 and 640 nm. Intensity profiles of the stains were generated from a line drawn through the center of the pellet and a sixth order smoothing curve (32 neighbors) was superimposed to capture and characterize distribution profiles of collagen matrix formation.

Micropellet biochemical analysis

Samples were thawed, lyophilized, weighed dry, and digested for 16 h at 56°C in proteinase K (MP Biomedicals) to assess DNA, glycosaminoglycan (GAG), and collagen content, as described previously²⁸.

Statistics

All statistical tests were performed in Statistica (Tulsa, OK). Cell Surface Marker Analysis: Three runs were averaged and presented as the mean expression $\pm 95\%$ CI. A one-way analysis of variance (ANOVA) with Tukey's HSD post-hoc test with $\alpha = 0.05$ and statistical significance set at $P \leq 0.05$ to compare CD73 expression across multiple passages. Galvanotaxis: Each data point represents the mean $\pm 95\%$ CI of 60–80 samples. A two-way ANOVA with Tukey's HSD post-hoc test ($\alpha = 0.05$) was performed on cell speed, directed velocity, and total displacement for factors of treatment (applied EF vs control), and passage number to determine significance ($P < 0.05$) of the effect of each factor and also the interaction of the factors. Chi square tests for linear trends were used to analyze the percentage of responding cells migrating in the cathodal direction. Micropellet Biochemical Analysis: Each data point represents the mean $\pm 95\%$ CI of five samples. Groups were examined for significant differences by two-way ANOVA with Tukey's HSD post-hoc test ($\alpha = 0.05$), with GAG, DNA, or collagen as the dependent variables, and passage number as the independent variable. Multiple correlation analyses were carried out to determine the dependence of cathodal migration on biochemical composition (GAG and collagen).

Results

Cell surface marker expression

The expression of cell surface markers in bovine SDSCs from P1 to P4 was evaluated by flow cytometry. Less than 3% of the analyzed population expressed CD31 or CD34 at any passage. Conversely,

CD49c and CD73 were expressed by a significant proportion of the cells. Expression of CD49c ($\alpha 3$ integrin) was stable and high ($>93\%$) during all passages. However, CD73 expression (ecto-5'-nucleotidase, SH3, SH4) showed a net change in expression from P1 (49.3%) to P4 (27.9%); CD73 expression initially increased from P1 to P2 ($P = 0.0128$) and then decreased at P3 and P4 ($P_{P3} = 0.0009$, $P_{P4} = 0.0002$), relative to P1 [Fig. 2].

EF-induced cell realignment and migration

Following exposure to an applied DC EF, the majority of cells reoriented their long axis perpendicular to the direction of the field; this orientation was not influenced by passage number [Fig. 3(a)]. The passage number of the cells, however, did directly influence the direction of induced migration. At P1, 85% of cells migrated primarily toward the positive pole (anode, Fig. 3(c)); by P4, nearly 70% of SDSCs had changed their direction of migration and moved toward the negative pole (cathode, Fig. 3(d)). A chi square test used to detect linear trends showed a significant decrease at each passage in cells migrating toward the anode [Fig. 4(b), $P < 0.0001$]. For comparison, control cells showed no significant bias toward either pole at all passages, ($57\% \pm 6.7$ toward the anode, $P = 0.13$ relative to 50%, Figs. 3(b) and 4(a)).

Cell migration parameters: speed and displacement depend on passage number

At all passages, SDSCs exposed to an applied DC EF traveled faster and migrated a further net distance than cells expanded similarly, but not exposed to a field ($P_{P1} = 0.0001$, $P_{P2} < 0.0001$, $P_{P3} = 0.0012$, $P_{P4} < 0.0001$, Fig. 5). Throughout passages P1–P4, the spontaneous migration displacement for control cells changed with passage number, initially increasing at P2 ($P < 0.0001$), before decreasing at P3 ($P = 0.0007$) and P4 ($P = 0.0021$), relative to P1. In contrast, spontaneous migration speed ($P_{P1-P2} = 0.15$; $P_{P1-P3} = 0.42$; $P_{P1-P4} = 0.57$) and directed velocity ($P_{P1-P2} = 0.98$; $P_{P1-P3} > 0.99$; $P_{P1-P4} = 0.99$) of control cells remained similar to passage P1. In contrast, for cells exposed to EF, there was a significant drop in speed ($P_{P1-P3} < 0.0001$, $P_{P1-P4} = 0.0203$) and directed velocity ($P_{P1-P3} < 0.0001$, $P_{P1-P4} < 0.0001$) at P3 and P4, relative to P1. The decreased trend in motility mirrors the decrease in CD73 surface marker expression observed after P2 ($P < 0.0001$), further highlighting the possibility of CD73 playing a role in cell migration.

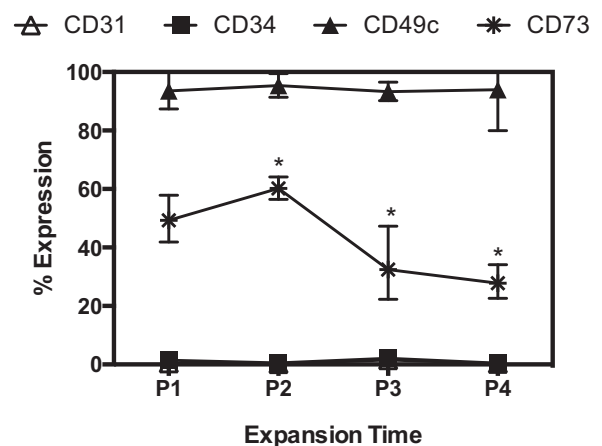


Fig. 2. Cell surface marker expression of CD31, CD34, CD49c, and CD73 over culture passage time in a growth factor cocktail. Each data point represents the mean $\pm 95\%$ CI expression of cells from three separate harvests. * $P < 0.05$ vs P1.

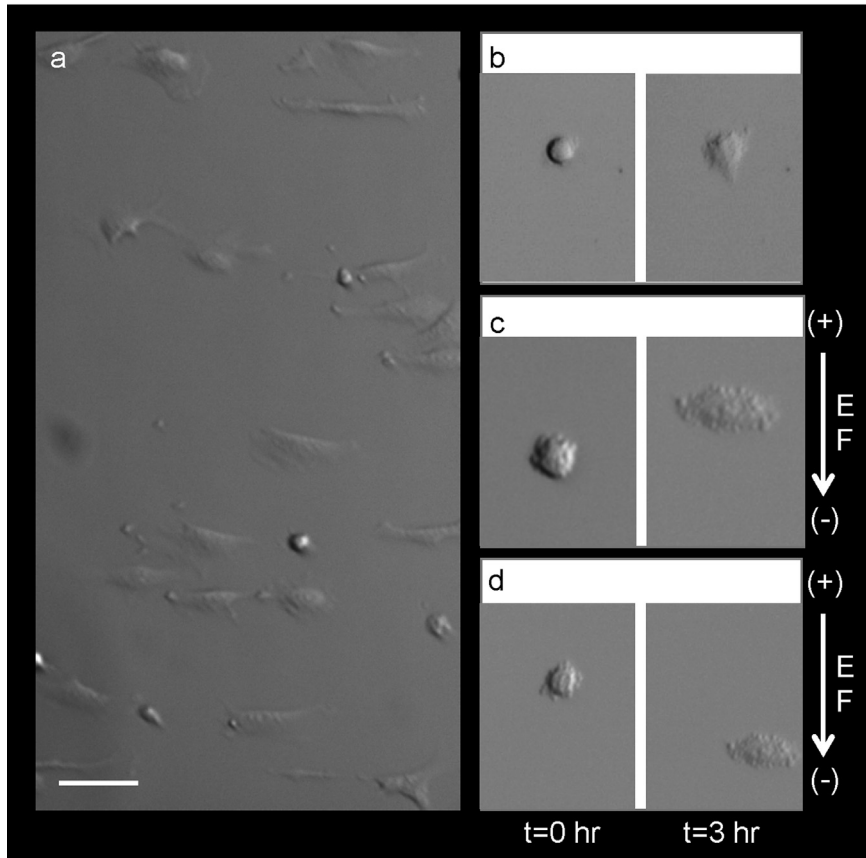


Fig. 3. (a) Representative endpoint ($t = 3$ h) EF cells with realignment of the long axis perpendicular to the direction of the field. Representative micrographs of (b) control cells and EF cells at (c) P1 and (d) P4. Final cell positions ($t = 3$ h, images on right of b–d) were compared to initial cell positions (images on left) and used to calculate overall displacement, speed, and directed velocity. Scalebar = $50 \mu\text{m}$.

This is further supported when P1 cells are exposed to APCP; a 65% reduction in cell speed ($16.0 \pm 2.13 \mu\text{m/h}$ vs $5.66 \pm 1.13 \mu\text{m/h}$) was noted ($n = 60$ cells/group, $P < 0.0001$).

Tissue development depends on passage number

ECM development from SDSC pellet culture was increasingly dependent on the extent to which cells had been expanded in a growth factor cocktail and the corresponding passage number. Pellets comprised of early passage cells (P1) elaborated significantly greater amounts of GAG/dw compared to pellets containing late

passage cells (P4) by day 28 ($16.3 \pm 1.89\%/dw$ vs $10.5 \pm 1.20\%/dw$, $P < 0.0001$) and this trend was consistent for day 42 ($20.2 \pm 3.64\%/dw$ vs $7.35 \pm 0.85\%/dw$, $P < 0.0001$, Fig. 6(a)). In fact, P1 pellets appeared to continue elaborating GAG following day 28, while P4 pellets began losing GAG content. In comparison, an opposing trend was noticed with collagen content; P4 pellets showed significantly increased amounts of collagen at all timepoints starting at day 14 relative to P1 pellets (day 14: $52.2 \pm 7.49\%/dw$ vs $11.2 \pm 2.77\%/dw$ ($P < 0.0001$); day 28: $43.5 \pm 8.65\%/dw$ vs $24.2 \pm 4.33\%/dw$ ($P < 0.0001$); day 42: $67.5 \pm 8.56\%/dw$ vs $27.1 \pm 4.50\%/dw$ ($P < 0.0001$), Fig. 6(b)).

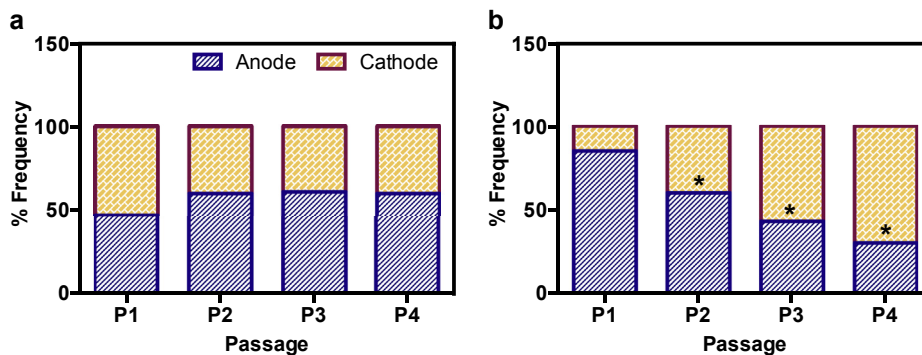


Fig. 4. Percentage of cells migrating toward the anode (positive pole) and the cathode (negative pole). (a) Control cells showed no significant difference in migration direction across all passages. (b) EF cells significantly changed direction with increasing passage. * $P < 0.0001$.

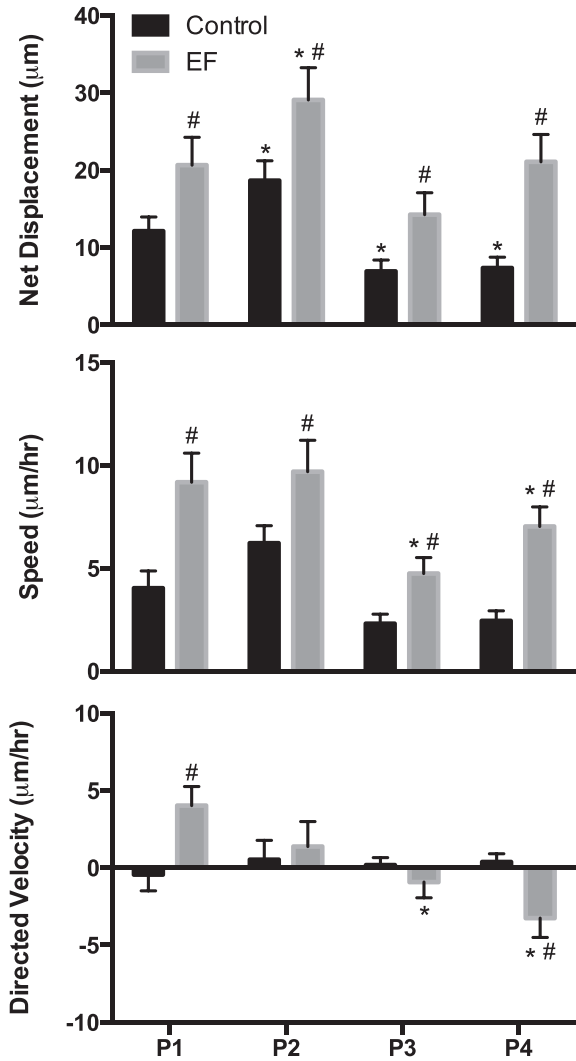


Fig. 5. Migration data from galvanotaxis studies performed for 3 h. *n* = 60–90 cells/run. **P* < 0.05 vs P1; [#]*P* < 0.05 vs control.

Substantial collagen II deposition occurs only in late passage SDSCs

Immunohistochemical staining revealed that collagen II deposition was more elaborate and consistent in P4 pellets than P1 pellets [Fig. 7(f) vs Fig. 7(b)]. Histograms of the gray value signal were constructed to quantify the distribution of the signal intensity through the diameter of the construct. These profiles confirm

nonhomogenous sinusoidal distribution of the signal intensity corresponding to the presence of collagen fibers initially at P1 [Fig. 7(d)] that fills in with increasing passage number to P4. The maintenance of signal intensity at an elevated gray value across the pellet confirms homogeneous distribution of collagen fibers [Fig. 7(h)]. Collagen I deposition was localized mainly to the periphery of all pellets [Fig. 7(a), (e)], evidenced by the increased signal intensity at the edges of the histogram, though was increasingly consistent for P4 pellets compared to their early counterparts [Fig. 7(g) vs Fig. 7(c)].

Chondrogenic phenotype correlates with cathodal migration

To understand the degree of association between biochemical constituents (GAG and collagen) elaborated by cells at each passage in pellet culture and the propensity of these same cells to migrate toward the cathode, a correlation analysis was performed. The results of this analysis show that GAG and collagen content can be useful predictors of cathodal migration potential ($r^2_{GAG} = 0.86$, $P = 0.07$; $r^2_{COL} = 0.92$, $P = 0.04$). When these two factors are taken in combination (i.e., multiple correlation), a strong significant correlation is found ($r^2 = 0.96$, $P = 0.02$).

Discussion

Previous studies examining passage-dependent changes to stem cell chondrogenesis have yielded mixed results; some studies have reported a maintenance of the chondrogenic potential in stem cells through multiple passages as high as 20²⁹, or even an increase in gene expression for positive markers of chondrogenesis (COL2A1 and AGC1) from early (P4) to late (P9) passages in adipose-derived stem cells³⁰. More often, studies have reported a decrease in chondrogenic potential with increased passage number^{31–34}, though in these studies, early passage was defined as cells that had undergone 3–5 trypsinizations. For comparison, our use of SDSCs through P4 falls within the timeframe reported to be high in chondrogenic potential, though there has been limited work exploring these nascent passages. To our knowledge, this is the first study to characterize the changing surface marker expression and migration pattern of SDSCs over time in culture through these 4 passages when chondrogenic potential is greatest. We have reported here that at early passages (P1, P2), cultured SDSCs exhibit anodal migration under EF strengths previously used to elicit galvanotaxis in chondrocytes. SDSCs switch their direction of migration on the same timescale, moving preferentially toward the cathode, just as permanently differentiated chondrocytes do.

SDSCs show considerable plasticity over extended passages; this plasticity is sufficient to change their migration direction in response to an applied EF. The SDSCs' changes in migratory

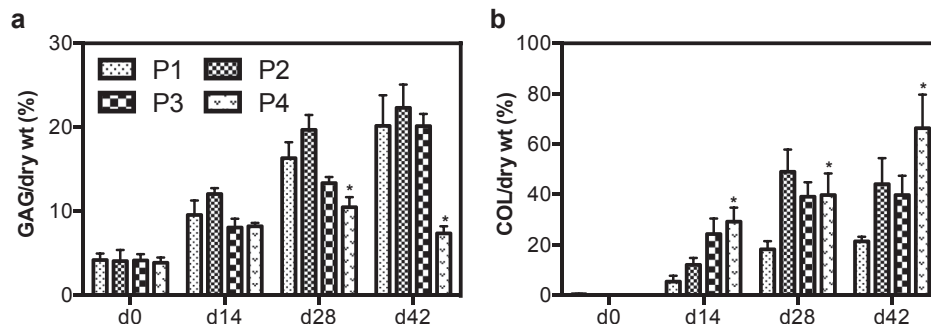


Fig. 6. Biochemical content [(a) GAG/dry wt and (b) COL/dry wt] of SDSC pellets from cells at different passages. *n* = 5 pellets/group, **P*_{P4} < 0.05 vs P1.

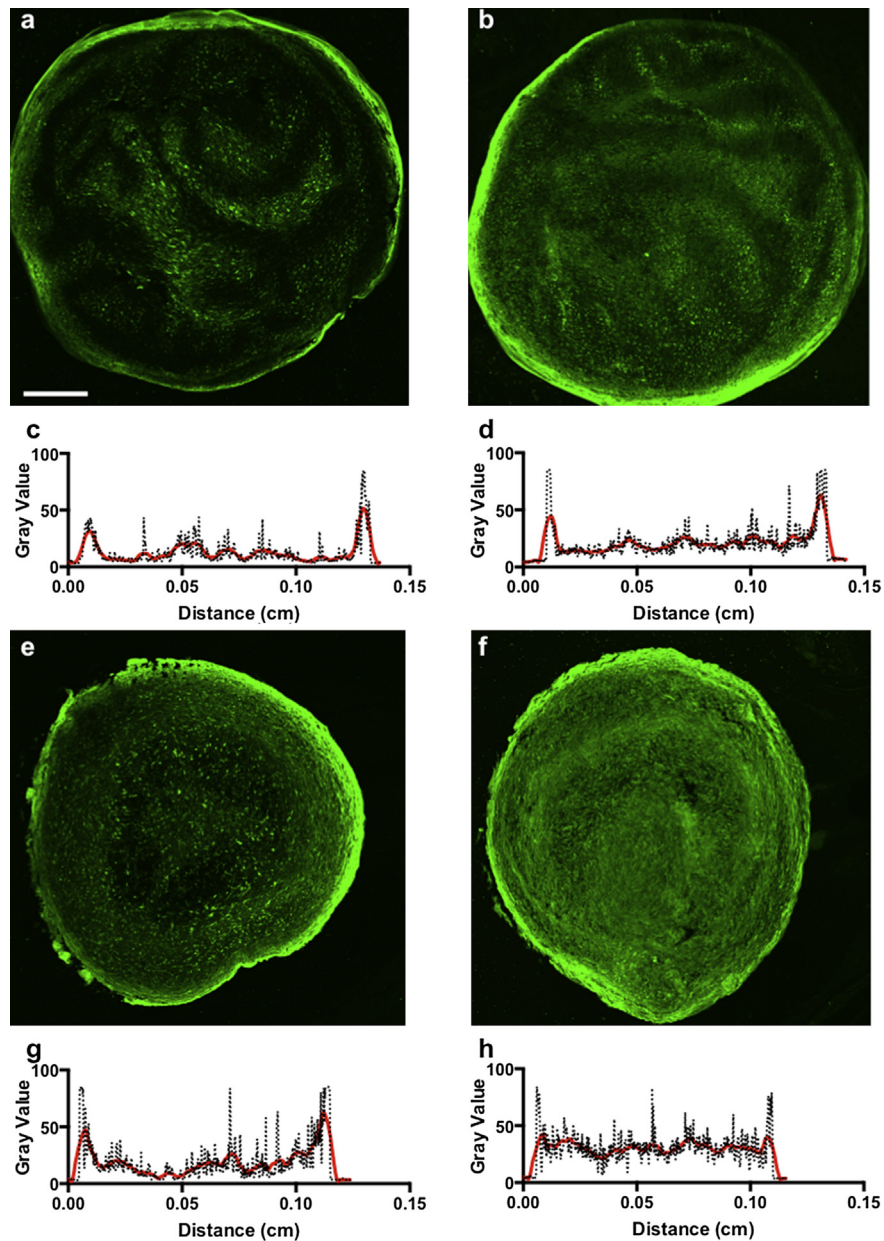


Fig. 7. Immunohistochemical stains of collagen I (a, e) and collagen II (b, f) for pellets comprised of P1 (top row) and P4 (bottom row) expanded cells. Histogram of the intensity profiles (c, d, g, h) through the center of the pellet reveal localized distribution patterns for each matrix component. Scalebar = 200 μm .

response to an applied EF may occur by one of several mechanisms. First, migration changes may be attributable to an altered differentiation state. During cell culture, SDSCs are exposed to a growth factor cocktail comprised of cytokines known to be responsible for driving differentiation or redifferentiation of cells toward a chondrocyte-like state³. In particular, progressive differentiation of the SDSCs can mediate not only changes in simple physical parameters of the culture but, as we show here, also expression of cell surface molecules.

Previous studies found that early passage MSCs share morphological characteristics with fibroblasts (elongated, flat cells³⁵). Further, both express N-cadherin and neural cell adhesion molecules (N-CAM)³⁶, key regulators of cell–cell interaction and cell migration³⁷. Additional exposure to growth factors brings about a chondrocyte differentiation process marked by distinct changes in cell morphology. Cells convert to a more spherical shape that

underlies varying physical traits known to influence motility. We also note that in late passage SDSCs, actin filaments appear dense and contracted, which may limit mobility and active migration. Alternatively, extended exposure to the growth factor cocktail may induce molecular changes to the cell surface of the differentiating cells. Indeed, flow cytometry revealed changes in surface molecules, although determining the role of CD73 and/or other candidate surface markers in mediating the EF responses will require further systematic study.

Expression of surface-associated proteins of chondrocytes (e.g., collagen II, keratin, sulfated proteoglycans) that are shed into the ECM surrounding the cells also increases with further expansion¹⁷. Changes in surface charge may be mediated by these surface-associated proteins, causing the cells to respond differently to the applied EF. Regulation of specific surface proteins can also change motility in EF-exposed cells. For example, the application of EF may

regulate and change the concentration of various ECM receptors for collagen and fibronectin, such as the $\alpha_2\beta_1$ integrin, which has been reported to be crucial for cell migration³⁸; these receptors polarize the integrin and its downstream effector RhoA to influence directionality of migration³⁹.

The altered migratory patterns we measured in SDSCs are likely to be initiated through changes in expression of cell surface markers, which accompanies increasing passages. We observed one such change, namely, a significant increase followed by decrease in the CD73 marker for stem cell expression. This initial increase in CD73 expression has previously been seen in mesenchymal stem cells derived from the synovium following P1⁴⁰, and other studies have reported a decrease in CD73 expression during chondrogenesis^{41–43}. This may be due in part to regulation of CD73 by cytokines and growth factors, such as TGF- β ⁴³. In addition to bolstering our previous hypothesis that the cells have adopted a more chondrocyte-like phenotype in P4 than in P1, these observations raise the possibility that CD73 or ecto-5'-nucleotidase, an enzyme that catalyzes the conversion of extracellular nucleotides to adenosine, plays a direct role in mounting a motility response to EF. Indeed, the observed motility decreases from P1–P4 support reports implicating CD73 in directly regulating cell migration⁴⁴. The results observed for P1 cells exposed to CD73 inhibitor further reinforce this.

Additionally, exogenously delivered factors such as bFGF⁴⁵ and PDGF- β ⁴⁶ have been found to modulate cell migration, perhaps as direct chemokinetic factors, similar to the roles of receptors for epidermal growth factor and hepatocyte growth factor during tumor invasion⁴⁷. Alternatively, components of the growth may alter motility via their capacity to upregulate the extracellular-signal-regulated kinase (ERK) and p38 mitogen-activated kinase (MAPK) signaling pathways⁴⁸. In fact, upregulation of the isoform 4 MAPK-1 protein has been shown for cells expanded in the same growth-factor cocktail as described here (ratio[SDSC Primed/SDSC Unprimed] \sim 2.4¹⁷). In keratinocytes and neutrophils, rapid and sustained phosphorylation of ERK, MAPK and Src is also a direct consequence of exposure to EF⁴⁹. In fact, activated Src kinase polarizes in the migration direction and recruits phosphatidylinositol 3,4,5-triphosphate (PIP3) to the leading edge of the cell, and targets the tumor suppressor phosphatase and tensin homologue (PTEN) to the lateral and back edges.

Although the primary responder(s) to the EF are still unknown, the PIP3 and PTEN redistributions are mediated by the Phosphatidylinositol 3-OH kinase- γ (PI(3)K γ) pathway and its upstream activators, receptor tyrosine kinases (RTK)⁴⁹. As such, it is reasonable to expect cells at different passages, which have been exposed to increased lengths of time of growth factor and binding to RTKs, will also exhibit varying responses to the applied EF. For example, an alteration or attenuation in the distribution of PIP3 and PTEN that is caused by altered growth factor exposure could shift the cells' migration direction. Taken together, previous studies, along with results presented here, point to the likelihood for growth factor priming and expansion to alter the behavior and response of the cells to external stimuli.

Late passage cells reveal the capacity to create cartilaginous-like tissue with increased expression of GAG and collagen by day 42. Surprisingly, however, these cells exhibited stunted GAG deposition that may be due to the abundance of elaborated collagen that, for the first time, nears native levels (\sim 60–70%/dry weight). This inverse relationship between GAG and collagen quantities follows trends noted previously for engineered cartilage⁵⁰. Confirmation of the presence of type II collagen at P4, the form predominantly found in articular cartilage, via immunohistological staining further suggests that only after multiple passages do cells possess a phenotype that resembles chondrocytes. Furthermore, from the

significantly strong correlation between collagen content and chondrocyte-like migration behavior (movement toward the cathode), we speculate that collagen II receptors and their associated $\alpha_{10}\beta_1$ integrins may be directly involved in directed movement.

There are some limitations to consider. First, in our studies, bovine SDSCs from skeletally immature animals were used, as they are readily available and well characterized. While their use facilitates comparisons of our current findings to our earlier work with juvenile bovine SDSCs³ and chondrocytes¹⁶, it is unclear if an older population of cells would respond similarly to exogenous cues. In wound conditions, it is also likely that a cytokine-rich environment would impart additional chemical factors that also could alter a cell's behaviors.

Nevertheless, our results show, for the first time, that the response of SDSCs to an applied DC EF is dependent upon the number of passages used to expand the cells in culture. Furthermore, the change in directionality that the cells exhibit, i.e., their migration toward opposite poles, is unique and has not been previously reported. A definitive characterization of SDSCs throughout the passages used to expand them may provide insights that will allow for optimization of their *in vivo* use in repair strategies. Ongoing work in the lab has begun characterizing the use of human bone marrow derived stem cells as well as human SDSCs for engineered cartilage in pellet culture. This progress, in addition to parallel studies examining the migratory potential of those cells, may further our understanding of how therapeutic modulation of exogenously applied EF can be used to accelerate and control cell migration during wound healing. Further studies are necessary, however, to elucidate the mechanism(s) behind the change in directionality of passaged SDSCs and to identify methods to control the motility process.

Author contributions

All authors contributed to the conception and design of the study, collection and analysis of data, drafting and revising the manuscript, and gave final approval of this submitted work. Two authors (ART, email: art2122@columbia.edu; CTH, email: cth6@columbia.edu) take responsibility for the integrity of the work as a whole.

Role of funding source

Research reported in this publication was supported in part by the National Institute of Arthritis and Musculoskeletal and Skin Diseases and National Institute of Biomedical Imaging and Bioengineering of the National Institutes of Health under Award Number R01AR46568, R01AR061988, P41EB002520. Funding was also provided by CDMRP Peer Reviewed Orthopedic Research Program (PRORP) Grant OR130124. The content is solely the responsibility of the authors and does not necessarily represent the official views of the National Institutes of Health or the Department of Defense. ART was supported by a National Science Foundation Graduate Fellowship.

Conflict of interest

The authors certify that there is no conflict of interest related to the work presented in this manuscript.

References

1. Mow VC, Bachrach NM, Setton LA, Guilak F. Stress, strain, pressure, and flow fields in articular cartilage and chondrocytes. In: Mow VC, Guilak F, Tran-Son-Tay R,

- Hochmuth RM, Eds. *Cell Mechanics and Cellular Engineering*. New York: Springer-Verlag; 1994:345–79.
2. Tew S, Redman S, Kwan A, Walker E, Khan I, Dowthwaite G, et al. Differences in repair responses between immature and mature cartilage. *Clin Orthop Relat Res* 2001;(Suppl 391): S142–52.
 3. Sampat SR, O'Connell GD, Fong JV, Alegre-Aguarón E, Ateshian GA, Hung CT. Growth factor priming of synovium-derived stem cells for cartilage tissue engineering. *Tissue Eng Part A* 2011;17(17–18):2259–65.
 4. Pei M, He F, Kish VL, Vunjak-Novakovic G. Engineering of functional cartilage tissue using stem cells from synovial lining: a preliminary study. *Clin Orthop Relat Res* 2008;466(8): 1880–9.
 5. Sampat SR, Dermksian MV, Oungouljian SR, Winchester RJ, Bulinski JC, Ateshian GA, et al. Applied osmotic loading for promoting development of engineered cartilage. *J Biomech* 2013;46(15):2674–81.
 6. Sakaguchi Y, Sekiya I, Yagishita K, Muneta T. Comparison of human stem cells derived from various mesenchymal tissues: superiority of synovium as a cell source. *Arthritis Rheum* 2005;52(8):2521–9.
 7. Koga H, Muneta T, Nagase T, Nimura A, Ju YJ, Mochizuki T, et al. Comparison of mesenchymal tissues-derived stem cells for in vivo chondrogenesis: suitable conditions for cell therapy of cartilage defects in rabbit. *Cell Tissue Res* 2008;333(2): 207–15.
 8. Yoshimura H, Muneta T, Nimura A, Yokoyama A, Koga H, Sekiya I. Comparison of rat mesenchymal stem cells derived from bone marrow, synovium, periosteum, adipose tissue, and muscle. *Cell Tissue Res* 2007;327(3):449–62.
 9. Hehenberger K, Heilborn JD, Brismar K, Hansson A. Inhibited proliferation of fibroblasts derived from chronic diabetic wounds and normal dermal fibroblasts treated with high glucose is associated with increased formation of l-lactate. *Wound Repair Regen Off Publ Wound Heal Soc Eur Tissue Repair Soc* 1998;6(2):135–41.
 10. Gunja N, Hung C, Bulinski J. Effects of DC electric fields on migration of cells of the musculoskeletal system. In: *Biological Effects of Electromagnetics*. CRC Press; 2011:185–200.
 11. Robinson KR. The responses of cells to electrical fields: a review. *J Cell Biol* 1985;101(6):2023–7.
 12. Soong HK, Parkinson WC, Bafna S, Sulik GL, Huang SC. Movements of cultured corneal epithelial cells and stromal fibroblasts in electric fields. *Invest Ophthalmol Vis Sci* 1990;31(11): 2278–82.
 13. Schengrund CL, Rosenberg A, Repman MA. Ecto-gangliosidase activity of herpes simplex virus-transformed hamster embryo fibroblasts. *J Cell Biol* 1976;70(3):555–61.
 14. Patel N, Poo MM. Orientation of neurite growth by extracellular electric fields. *J Neurosci* 1982;2(4):483–96.
 15. Finkelstein EI, Chao PHG, Hung CT, Bulinski JC. Electric field-induced polarization of charged cell surface proteins does not determine the direction of galvanotaxis. *Cell Motil Cytoskeleton* 2007;64(11):833–46.
 16. Chao PH, Roy R, Mauck RL, Liu W, Valhmu WB, Hung CT. Chondrocyte translocation response to direct current electric fields. *J Biomech Eng* 2000;122(3):261–7.
 17. Alegre-Aguarón E, Sampat SR, Xiong JC, Colligan RM, Bulinski JC, Cook JL, et al. Growth factor priming differentially modulates components of the extracellular matrix proteome in chondrocytes and synovium-derived stem cells. *PLoS One* 2014;9(2):e88053.
 18. Chamberlain G, Fox J, Ashton B, Middleton J. Concise review: mesenchymal stem cells: their phenotype, differentiation capacity, immunological features, and potential for homing. *Stem Cells* 2007;25(11):2739–49.
 19. Fan J, Varshney R, Ren L, Cai D, Wang D. Synovium-derived mesenchymal stem cells: a new cell source for Musculoskeletal Regeneration. *Tissue Eng Part B Rev* 2009;15(1):75–86.
 20. Dominici M, LeBlanc K, Mueller I, Slaper-Cortenbach I, Marini F, Krause D, et al. Minimal criteria for defining multipotent mesenchymal stromal cells. The International Society for Cellular Therapy position statement. *Cytotherapy* 2006; 8(4):315–7.
 21. Grogan SP, Barbero A, Diaz-Romero J, Cleton-Jansen AM, Soeder S, Whiteside R, et al. Identification of markers to characterize and sort human articular chondrocytes with enhanced in vitro chondrogenic capacity. *Arthritis Rheum* 2007;56(2):586–95.
 22. Lee HJ, Choi BH, Min BH, Park SR. Changes in surface markers of human mesenchymal stem cells during the chondrogenic differentiation and dedifferentiation processes in vitro. *Arthritis Rheum* 2009;60(8):2325–32.
 23. Cho SY, Polster J, Engles JM, Hilton J, Abraham EH, Wahl RL. In vitro evaluation of adenosine 5'-monophosphate as an imaging agent of tumor metabolism. *J Nucl Med Off Publ Soc Nucl Med* 2006;47(5):837–45.
 24. Gunja NJ, Dujari D, Chen A, Luengo A, Fong JV, Hung CT. Migration responses of outer and inner meniscus cells to applied direct current electric fields. *J Orthop Res* 2012;30(1): 103–11.
 25. Chao PHG, Lu HH, Hung CT, Nicoll SB, Bulinski JC. Effects of applied DC electric field on ligament fibroblast migration and wound healing. *Connect Tissue Res* 2007;48(4):188–97.
 26. Bian L, Lima EG, Angione SL, Ng KW, Williams DY, Xu D, et al. Mechanical and biochemical characterization of cartilage explants in serum-free culture. *J Biomech* 2008;41(6): 1153–9.
 27. Kelly TAN, Wang CCB, Mauck RL, Ateshian GA, Hung CT. Role of cell-associated matrix in the development of free-swelling and dynamically loaded chondrocyte-seeded agarose gels. *Biorheology* 2004;41(3–4):223–37.
 28. Riesle J, Hollander AP, Langer R, Freed LE, Vunjak-Novakovic G. Collagen in tissue-engineered cartilage: types, structure, and crosslinks. *J Cell Biochem* 1998;71(3):313–27.
 29. Yoo JU, Barthel TS, Nishimura K, Solchaga L, Caplan AI, Goldberg VM, et al. The chondrogenic potential of human bone-marrow-derived mesenchymal progenitor cells. *J Bone Jt Surg Am Vol* 1998;80(12):1745–57.
 30. Estes BT, Wu AW, Storms RW, Guilak F. Extended passaging, but not aldehyde dehydrogenase activity, increases the chondrogenic potential of human adipose-derived adult stem cells. *J Cell Physiol* 2006;209(3):987–95.
 31. Kretlow JD, Jin YQ, Liu W, Zhang WJ, Hong TH, Zhou G, et al. Donor age and cell passage affects differentiation potential of murine bone marrow-derived stem cells. *BMC Cell Biol* 2008;9(1):60.
 32. Tan Q, Lui PPY, Rui YF. Effect of in vitro passaging on the stem cell-related properties of tendon-derived stem cells—implications in tissue engineering. *Stem Cells Dev* 2012;21(5):790–800.
 33. Vacanti V, Kong E, Suzuki G, Sato K, Canty JM, Lee T. Phenotypic changes of adult porcine mesenchymal stem cells induced by prolonged passaging in culture. *J Cell Physiol* 2005;205(2):194–201.
 34. Wang M, Rahnama R, Cheng T, Grotkopp E, Jacobs L, Limburg S, et al. Trophic stimulation of articular chondrocytes by late-passage mesenchymal stem cells in coculture. *J Orthop Res Off Publ Orthop Res Soc* 2013;31(12):1936–42.

35. Alt E, Yan Y, Gehmert S, Song YH, Altman A, Gehmert S, *et al.* Fibroblasts share mesenchymal phenotypes with stem cells, but lack their differentiation and colony-forming potential. *Biol Cell Under Auspices Eur Cell Biol Organ* 2011;103(4): 197–208.
36. DeLise AM, Fischer L, Tuan RS. Cellular interactions and signaling in cartilage development. *Osteoarthr Cartil* 2000;8(5):309–34.
37. Eggers K, Werneburg S, Schertzinger A, Abeln M, Schiff M, Scharenberg MA, *et al.* Polysialic acid controls NCAM signals at cell-cell contacts to regulate focal adhesion independent from FGF receptor activity. *J Cell Sci* 2011;124(Pt 19):3279–91.
38. Etienne-Manneville S, Hall A. Integrin-mediated activation of Cdc42 controls cell polarity in migrating astrocytes through PKCzeta. *Cell* 2001;106(4):489–98.
39. Tsai CH, Lin BJ, Chao PHG. $\alpha 2\beta 1$ integrin and RhoA mediates electric field-induced ligament fibroblast migration directionality. *J Orthop Res* 2012;31(2):322–7.
40. Jo CH, Ahn HJ, Kim HJ, Seong SC, Lee MC. Surface characterization and chondrogenic differentiation of mesenchymal stromal cells derived from synovium. *Cytotherapy* 2007;9(4): 316–27.
41. Delorme B, Ringe J, Gallay N, Le Vern Y, Kerboeuf D, Jorgensen C, *et al.* Specific plasma membrane protein phenotype of culture-amplified and native human bone marrow mesenchymal stem cells. *Blood* 2008;111(5):2631–5.
42. Song L, Webb NE, Song Y, Tuan RS. Identification and functional analysis of candidate genes regulating mesenchymal stem cell self-renewal and multipotency. *Stem Cells* 2006;24(7):1707–18.
43. Ode A, Schoon J, Kurtz A, Gaetjen M, Ode JE, Geissler S, *et al.* CD73/5'-ecto-nucleotidase acts as a regulatory factor in osteo-/chondrogenic differentiation of mechanically stimulated mesenchymal stromal cells. *Eur Cells Mater* 2013;25: 37–47.
44. Ode A, Kopf J, Kurtz A, Schmidt-Bleek K, Schrade P, Kolar P, *et al.* CD73 and CD29 concurrently mediate the mechanically induced decrease of migratory capacity of mesenchymal stromal cells. *Eur Cells Mater* 2011;22:26–42.
45. Maniwa S, Ochi M, Motomura T, Nishikori T, Chen J, Naora H. Effects of hyaluronic acid and basic fibroblast growth factor on motility of chondrocytes and synovial cells in culture. *Acta Orthop Scand* 2001;72(3):299–303.
46. Schmidt MB, Chen EH, Lynch SE. A review of the effects of insulin-like growth factor and platelet derived growth factor on in vivo cartilage healing and repair. *Osteoarthr Cartil OARS Osteoarthr Res Soc* 2006;14(5):403–12.
47. Wells A. Tumor invasion: role of growth factor-induced cell motility. *Adv Cancer Res* 2000;78:31–101.
48. Giuliani R, Bastaki M, Coltrini D, Presta M. Role of endothelial cell extracellular signal-regulated kinase1/2 in urokinase-type plasminogen activator upregulation and in vitro angiogenesis by fibroblast growth factor-2. *J Cell Sci* 1999;112(Pt 15): 2597–606.
49. Zhao M, Song B, Pu J, Wada T, Reid B, Tai G, *et al.* Electrical signals control wound healing through phosphatidylinositol-3-OH kinase-gamma and PTEN. *Nature* 2006;442(7101): 457–60.
50. Bian L, Angione SL, Ng KW, Lima EG, Williams DY, Mao DQ, *et al.* Influence of decreasing nutrient path length on the development of engineered cartilage. *Osteoarthr Cartil OARS Osteoarthr Res Soc* 2009;17(5):677–85.